Journal of Solid State Chemistry 184 (2011) 1638–1643

Contents lists available at ScienceDirect

Journal of Solid State Chemistry

journal homepage: www.elsevier.com/locate/jssc

Facile synthesis of Cu_2O nanocube/polycarbazole composites and their high visible-light photocatalytic properties

Wei Sun, Wendong Sun *, Yujiang Zhuo, Ying Chu *

Department of Chemistry, Northeast Normal University, Changchun 130024, PR China

ARTICLE INFO

Article history:
Received 28 December 2010
Received in revised form
27 March 2011
Accepted 29 March 2011
Available online 27 April 2011

Keywords:
Cu_2O/polycarbazole
Nanocube
Composite
Photocatalyst

ABSTRACT

Cu_2O nanocube/polycarbazole composites have been prepared by an one-pot solvothermal process using carbazole as a reductant. The polycarbazole layer not only protected and stabilized Cu_2O particles, but also prohibited the recombination of photogenerated electrons–holes pair and facilitated interfacial charge transfer between polycarbazole and Cu_2O. The composition, structure and morphology of the obtained products was systematically studied by X-ray powder diffraction (XRD), Field-emission scanning electron microscopy (FE-SEM), High-resolution transmission electron microscopy (HRTEM), Fourier transformation infrared spectroscopy (FT-IR), X-ray photoelectron spectroscopy (XPS) and UV–visible spectrophotometer. Furthermore, the visible-light photocatalytic behavior of the Cu_2O nanocube/polycarbazole composites on the methyl orange was investigated.

1. Introduction

In recent years, photocatalysis has attracted much attention because it is a relatively new wastewater treatment and purification technology with many advantages, such as complete degradation, efficient and stable process, and sunlight availability. Therefore, the rapid developing photocatalytic oxidation technology provides a new way to solve the increasingly serious water, air, and soil pollution. Currently, photocatalytic degradation mainly takes advantage of special electronic structure and photochemical properties of semiconductors. For the above reasons, a large number of materials could be used as photocatalysts, such as TiO_2 and ZnO [1,2]. It is a pity that both of them are active under ultraviolet or near-ultraviolet radiation that occupies only a fraction of the solar light. Consequently, to obtain highly efficient visible light photocatalytic materials is of great importance. Materials with a good light activity, light stability, photocatalytic efficiency, or visible light-sensitive have been the goal that is pursued by many scientists.

Cuprous oxide (Cu_2O) is a p-type semiconductor with a direct band gap of 2.17 eV. Owing to the quantum size effects, Cu_2O nanoparticles show many particular optical, electrical, and photoelectrochemical properties. Recently, Cu_2O has aroused much interest owing to its potential applications for conversion of solar energy [3], electrode materials [4], sensors [5], and photocatalyst for degradation of organic pollutants [6]. Because the shape and size of inorganic materials directly affect their physical and chemical properties, many efforts have been devoted to the synthesis of uniformed cuprous oxide with various structure and morphologies during the past decade [7–14]. For example, Kim et al. [7] used chloride to direct the morphology of Cu_2O nanostructures by reducing copper nitrate with ethylene glycol heated to 140 °C in the presence of PVP. Chen et al. [8] prepared hex-pod-like Cu_2O whiskers from a $Cu(CH_3COO)_2$ precursor under hydrothermal conditions. However, electron–hole pairs can easily recombine and the photochemical reaction is possible inhibited when the narrow gap semiconductor (i.e., Cu_2O) is used as a photocatalyst [15,16]. For example, Zhou group [17] found that the coexistence of Cu_2O and Cu in the nanoparticle was propitious to the high photocatalytic activity owing to their heterojunction effect. On the other hand, Cu_2O particles are easy to aggregate or be oxidized. In order to solve this problem, construction of Cu_2O complex with noble metal, other semiconductors or conductive materials may be a good way [15]. Hydrazine [10], sodium borohydride [11], ethylene glycol [12] or glucose [13] is frequently used as the reductant to synthesize Cu_2O particles, but rare report is found using carbazole monomers as reductants except that Zahoor and co-workers [18] reported cations assisted oxidative polymerization of carbazole to form Ag@polycarbazole nanocomposite materials. Actually, polycarbazole is a relatively new conductive polymer, which has been attracted increasing interest because of its potential application in hole-transporting and photoconductivity fields [19,20]. In addition, polycarbazole as a conjugated polymer with semiconducting behavior can be used in electronic and optoelectronic devices [21]. Thus, we considered that the conductive polymer shell might facilitate the separation

* Corresponding authors. Fax: +86 431 85098768.
E-mail addresses: sunwd843@nenu.edu.cn (W. Sun), chuying@nenu.edu.cn (Y. Chu).

0022-4596/$ - see front matter © 2011 Elsevier Inc. All rights reserved.
doi:10.1016/j.jssc.2011.03.055

of photogenerated electron–hole pairs. Polycarbazole was usually synthesized by electrochemical deposition [19]. Herein, we obtained Cu_2O/polycarbazole nanocube composites using carbazole monomers as reductants through chemical polymerization. Though Cu_2O nanocrystals with various morphologies have been successfully achieved, the reports about the controlled synthesis of the Cu_2O nanocube/polycarbazole composites and the corresponding investigation on its photocatalytic properties are limited [9]. Compared with electrochemical deposition, our method favors environmental conservation and energy conservation. Polycarbazole can form a protective layer on the surface of Cu_2O, which also improves the separation of electron–hole pairs and electron utilization between polycarbazole and Cu_2O.

2. Experimental section

2.1. Preparation of the Cu_2O nanocube/polycarbazole composites

All the chemical reagents were of analytical grade and were used as received. In a typical experiment, sodium hydroxide (1.6 mmol), PVP (0.5 g) and carbazole (0.8 mmol) were mixed into a anhydrous ethanol (35 mL). This solution was stirred for 2 h at room temperature to ensure that they were dissolved completely. Then, $Cu(NO_3)_2 \cdot 3H_2O$ (0.8 mmol) were dissolved in the above solution under stirring for another 30 min. The blue precipitate suspension appeared soon. After that, the obtained solution was transferred into a 50 mL Teflon-lined autoclave and heated at 160 °C for 18 h. Finally, the products were washed with distilled water and ethanol for several times, and then dried at 60 °C for 12 h in vacuum. After that, the product was collected as sample 1 for further characterization. For comparison, a control experiment without PVP under otherwise the same conditions was carried out and the product was labeled as sample 2.

2.2. Photocatalysis

Photocatalytic activity of the Cu_2O nanocube/polycarbazole composites and pure Cu_2O (Supplementary data A and B) was examined by measuring the reduction rate of the methyl orange (MO). First, catalysts (8 mg) were dispersed in a MO solution (40 mL, 20 mg/L) for 60 min in dark to obtain absorption equilibrium. Then, the suspension exposed to light from the visible lamp and the photocatalytic reaction started. At certain intervals, the reaction suspension (3 mL) was taken out, centrifuged at 8000 rpm for 10 min. Finally, the supernatant was analyzed. The concentration of the MO was tracked by UV–visible absorption spectrophotometer.

2.3. Characterization

The X-ray powder diffraction (XRD) pattern of the products were performed using a Rigaku X-ray diffractometer with Cu $K\alpha$ radiation ($\lambda = 1.5406$ Å). The morphology of the products were observed by Field-emission scanning electron microscopy (FE-SEM, JEOL 7500B), high-resolution transmission electron microscopy (HRTEM, JEM-2100) with an accelerating voltage of 200 kV and transmission electron microscopy (TEM, Hitachi H-800). The X-ray photoelectron spectroscopy measurement (XPS) was carried out by thermo ESCALAB 250. UV–visible absorption was recorded on a SHIMADZU UV-2550 UV–visible spectrophotometer. Photocatalytic reaction was carried out with a 300 W xenon lamp as the visible-light source at room temperature.

3. Results and discussion

The crystal structure and chemical composition of the as-obtained samples were examined by powder X-ray diffraction (XRD) and the XRD patterns of Cu_2O nanocrystals from different conditions are shown in Fig. 1. The diffraction peaks in Fig. 1 (A and B) can be indexed to cube phase Cu_2O (JCPDS no. 05-0667), including both peak position and their relative intensity. The broad peak centered at $2\theta = 23^\circ$ can be attributed to the organic phase in these two curves [22]. Because no PVP is used in sample 2, and the broad peak was different from the characteristic peak of commercial carbazole monomers (Supplementary data C), it is surmised that the broad peak in Fig. 1 (A and B) can be assigned to the amorphous polycarbazole.

The morphologies of the obtained samples are shown in Fig. 2. TEM image in Fig. 2(a) shows that sample 1 is composed of cubes with diameter of about 80 nm and the surface of cuprous oxide is decorated with a shell, which can be seen clearly in a larger magnification as shown in inset of Fig. 2(a). Fig. 2(b) depicts the lattice fringes of Cu_2O nanocubes and the fringe spacing is measured as 0.21 nm, which is in good agreement with the (2 0 0) lattice spacing of Cu_2O [23]. The Fast Fourier Transform (FFT) pattern in inset of Fig. 2(b) reveals that the cubic Cu_2O is actually single-crystal. To understand the effect of PVP on the formation of Cu_2O nanocubes, control experiment without PVP was carried out, and the result showed that the obtained cubes were dispersed unevenly (Fig. 2c). This proves that PVP acts as a colloidal dispersant agent in the system. On the other hand, when the amount of NaOH was increased, spherical copper particles was achieved. Thus, we expect that NaOH plays an important role on the formation of the Cu_2O nanocube/polycarbazole composites.

Further morphological characterization of Cu_2O samples was performed by SEM. The SEM image of sample 1 in Fig. 3(a) shows a panoramic view of the products, from which Cu_2O nanocubes with narrow size distribution are demonstrated. The image shows that the cubic cuprous oxide crystal is bounded by six (1 0 0) surfaces. The (1 0 0) facet of cuprous oxide nuclei is polar whereas (1 1 1) facet is nonpolar [8]. We speculate that some interactions exist between nitrogen atoms of polycarbazole and the (1 0 0) facets of the cubic Cu_2O crystal, such as physical adsorption or chemical bonding, that may kinetically favor the preferential crystal growth along the (1 1 1) direction of the cubic Cu_2O crystal, and the facets with a slower growth rate would be

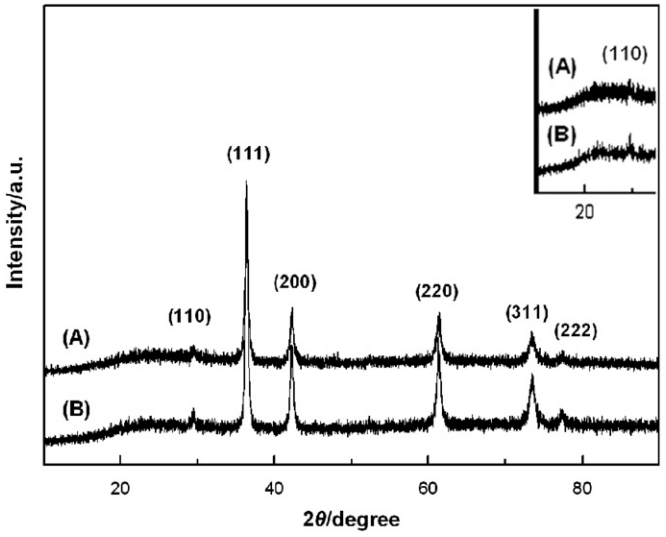

Fig. 1. XRD patterns of sample 1 (A), sample 2 (B) and inset is partial enlargement of this picture.

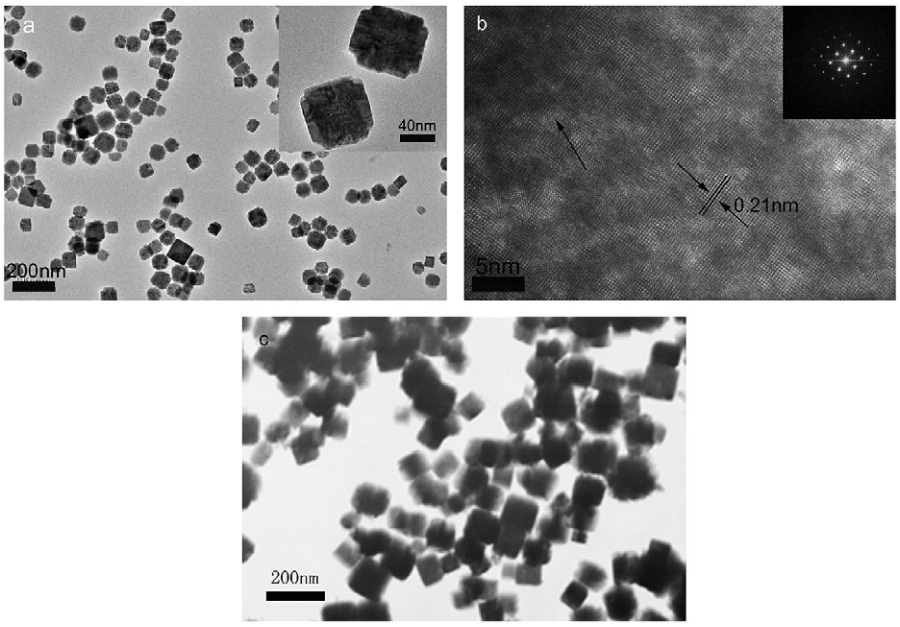

Fig. 2. TEM images of sample 1 (a) and sample 2 (c); HRTEM images of sample 1 (b).

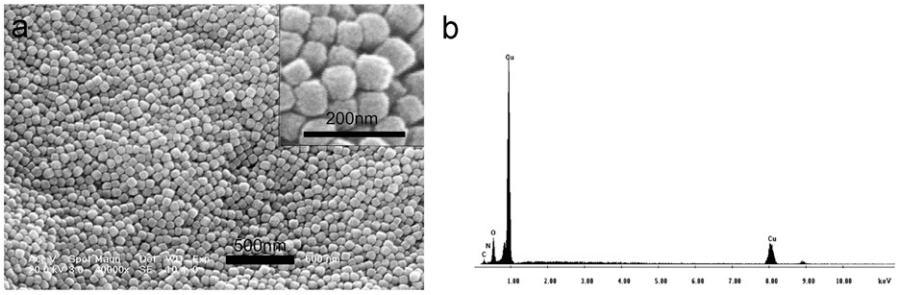

Fig. 3. Field-emission scanning electron microscopy (FESEM) images (a) and EDX pattern of sample 1 (b).

exposed more on the crystal surface [9]. The corresponding energy-dispersive X-ray (EDX) analysis (Fig. 3b) shows that the atomic ratio of copper and oxygen is close to 2:1 in the spectrum, confirming that the obtained products are Cu_2O crystals. Apart from the strong signals from the copper element, weak signals from the C and N are recorded. Based on the above analysis, we can come to a primary conclusion that the obtained products are composed of Cu_2O and polycarbazole.

The polycarbazole as a coating material over Cu_2O nanocubes was further characterized by FT-IR (Fig. 4). The bands presented at 3433, 1632, and 1417 cm^{-1} relate to N–H stretching, aromatic ring stretching, and C–N stretching vibrations, respectively [24]. The peak appearing at 857 cm^{-1} is the characteristic band for 3, 6 polycarbazole [24,25]. The peak at 625 cm^{-1} belongs to the characteristic peak of cuprous oxide [26]. We also investigated the UV–visible absorption characteristics of the Cu_2O nanocube/polycarbazole composites and the result is presented in Fig. 5. The characteristic absorption peaks at 292, 348 and 451 nm are observed. The first two peaks are belong to polycarbazole, which is found to red-shift in comparison to the monomer peaks at 289 and 325 nm [25], and the weak bands near 451 nm correspond to the absorption peak of Cu_2O [27]. These datum further elucidated that polycarbazole exists.

To further investigate the surface composition of the as-prepared Cu_2O nanocube/polycarbazole composites, sample 1 is characterized via XPS. The peaks situated at 284.6, 286.7, and 288.3 eV can be attributed to C–C, C–N, and C═O vibration,

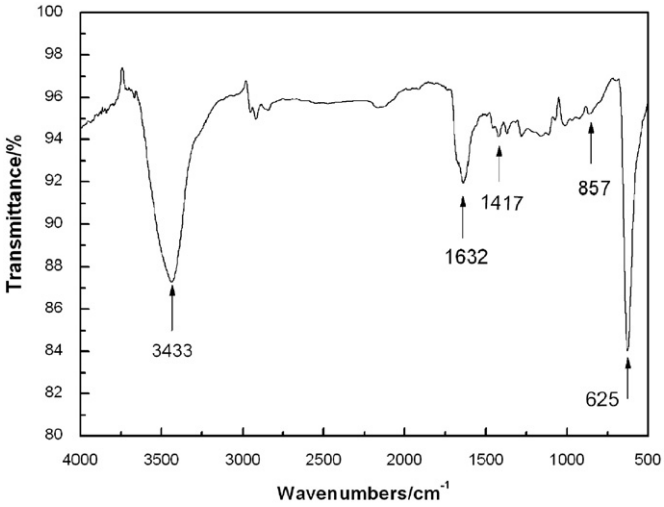

Fig. 4. FT-IR spectrum of sample 1.

respectively (Fig. 6a) [28]. The main peak at 399.3 eV is corresponding to the C–N bond of carbazole in Fig. 6(b), which has been studied by both Taoud group [29] and Abe et al. [30]. The binding energy of nitrogen exhibits that polycarbazole exists on the surface of cuprous oxide. Fig. 6(c) presents the photoelectron spectrum of Cu. The peak at 932.50 eV, corresponding to the

binding energy of $Cu_{3/2,2P}$, is in good agreement with data observed for Cu_2O [15]. As shown in Fig. 6(d), the O_{1S} core-level spectrum is broad, and three O_{1S} peaks (marked as A, B and C) are resolved through a curve-fitting procedure. Peak (A), at the lower energy of 530.18 eV, agrees with O in Cu_2O [15]; Peak (B), located at 531.56 eV, is attributed to the carbonyl oxygen [28,29]; Peak (C) at 532.9 eV is attributed to oxygen adsorbed on the surface of Cu_2O nanocubes [31]. These results indicate that polycarbazole exists as a coating material.

Photocatalytic activities of the as-obtained cuprous oxide crystals were investigated towards the MO solution at room temperature. Fig. 7(a) and (b) represent the relationships between irradiation time and absorbance at 460 nm of the MO solution by using the Cu_2O nanocube/polycarbazole composites (sample 1) and pure Cu_2O as catalysts, respectively. The dependence of the MO concentration on reaction time over the Cu_2O nanocube/polycarbazole composites and pure Cu_2O is shown in Fig. 7(c) and (d), respectively. Prior to irradiation, the MO solution mixed with the catalyst was kept in the dark for 60 min to obtain absorption equilibrium. In Fig. 7, degradation rate of the MO solution (sample 1) reaches 83.6% in 120 min, while it is only 30.1% in the presence of pure Cu_2O under the same conditions. Thus, pure Cu_2O nanocube is not a good catalyst for degradation of the MO, and a similar phenomena was also found in some reports [9,32]. Xu group [9] found that Cu_2O octahedra showed much higher activity than cubes. Ho and Huang [32] reported that Cu_2O nanocube exhibited lower photocatalytic activity toward the photodegradation of the MO. While we obtained Cu_2O nanocubes covered by polycarbazole, the activity of Cu_2O nanocubes was enhanced. The photodegradation mechanism is presented as follows.

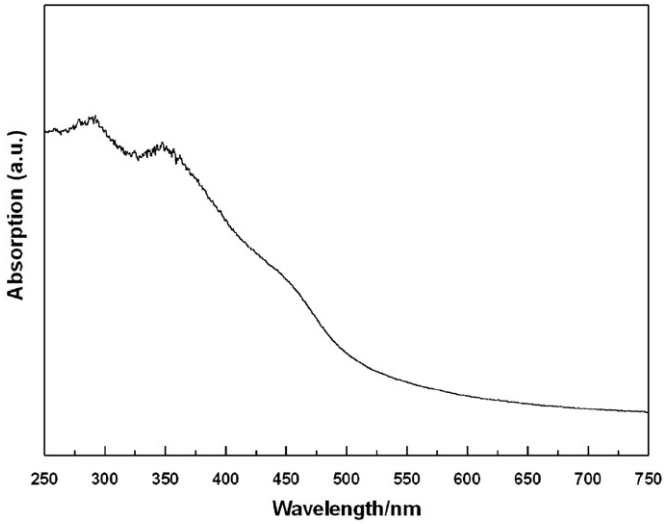

Fig. 5. UV–visible absorption spectrum of sample 1.

As known to all, the adsorption ability and the separation of photogenerated electrons–holes pair influenced the photocatalytic efficiency of the photocatalyst. As covered by a crude polycarbazole, the adsorption ability of Cu_2O for the MO was improved. Furthermore, when the photoelectron energy is greater than the band gap, optical excitation electrons transfer from the valence band to the conduction band and electrons (e^-) and holes (h^+) are produced. Hole has strong oxidizability, and electron has strong reducibility. Therefore, active electrons and holes have the capacity to reduce and oxidize substances absorbed on photocatalyst surface. Due to the characteristic of p-type semiconducting, Cu_2O depend mainly on holes conductance, while polycarbazole as a conjugated polymer is easy to accept electrons [18,19,33]. When Cu_2O and polycarbazole are combined together, electron excited on the surface of Cu_2O could be dispersed to polycarbazole, which may restrain the combination of the electrons–holes pairs and

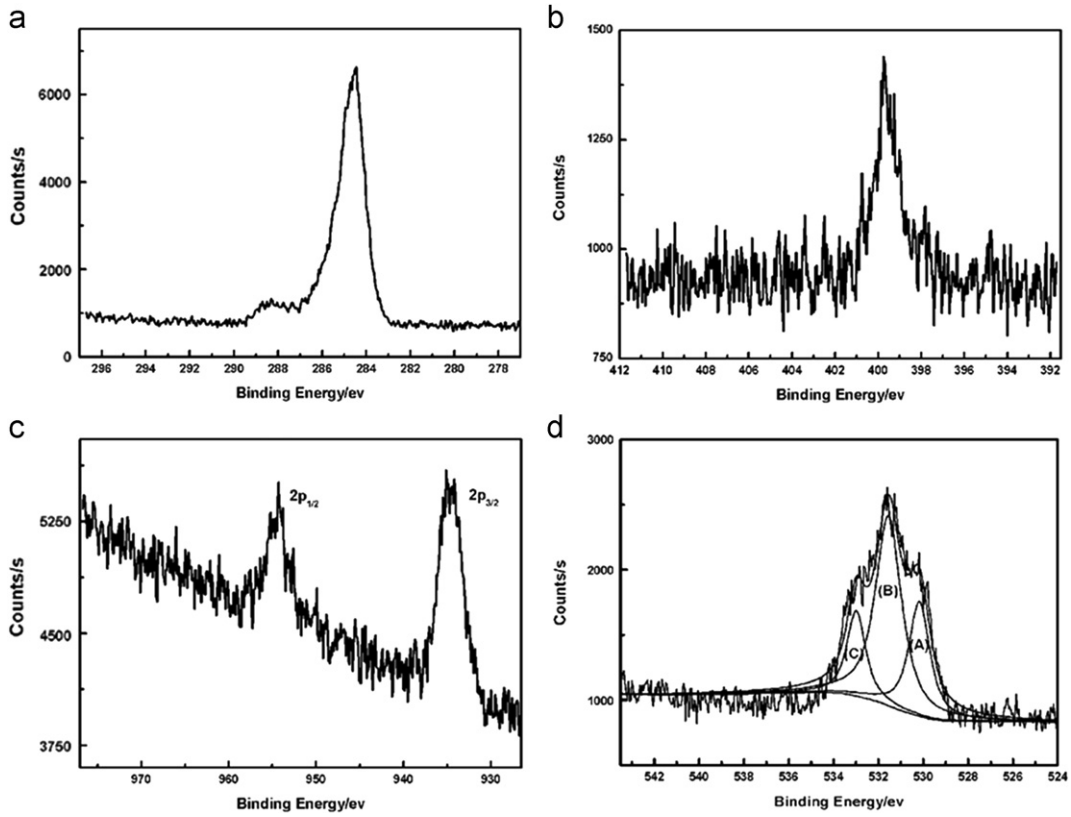

Fig. 6. XPS patterns of sample 1: C_{1S} spectra (a), N_{1S} spectra (b), Cu_{2P} spectra (c), and O_{1S} spectra by curve-fitting (d).

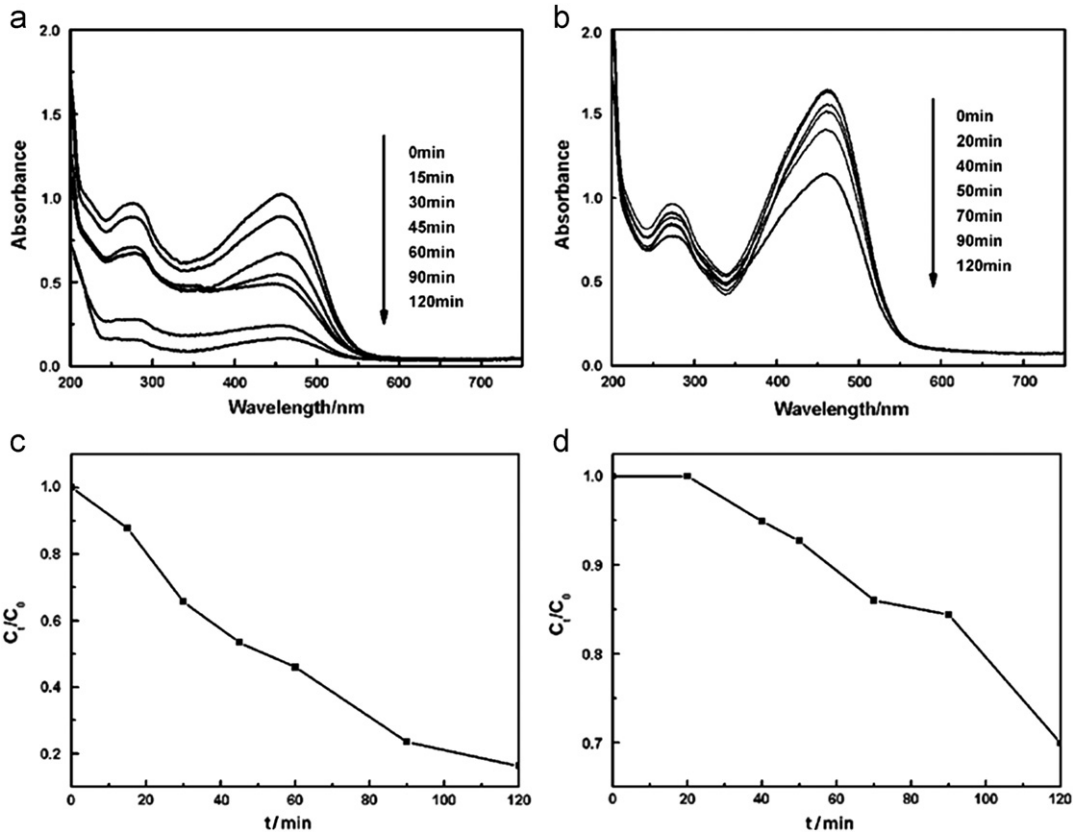

Fig. 7. Photocatalytic degradation of methyl orange (20 mg/L, 40 mL) under visible-light in the presence of: sample 1 (a and c, 8 mg) and pure Cu_2O (b and d, 8 mg), respectively.

improve the photocatalytic activity of the Cu_2O nanocube/polycarbazole composites. In other words, the oxidation sites are mainly on Cu_2O and the reduction sites are mainly dominated by polycarbazole. The formation of composite is energetically favorable for the separation of the electrons–holes pairs and interfacial charge transfer between Cu_2O and polycarbazole. As molecular O_2 is easy to be adsorbed, electrons accumulated on polycarbazole could be captured by O_2 to yield O_2^- [34]. Then, O_2^- further react with electrons and H_2O to produce hydrogen peroxide (H_2O_2) and hydroxyl radical (•OH), which could effectively degrade the MO solution [34]. As a result, the photocatalytic activity of Cu_2O nanocube/polycarbazole composites was improved, which is attributed to the good adsorption ability of the composite and the separation of photogenerated electrons–holes pair between Cu_2O and polycarbazole.

4. Conclusions

In summary, the Cu_2O nanocube/polycarbazole composites with high visible-light photocatalytic activity have been successfully prepared via an one-pot solvothermal process with carbazole as reductants. The Cu_2O nanocubes have structure with size around 80 nm with the surface layer of a thin rough polycarbazole. Coating on the Cu_2O nanocubes, polycarbazole plays two important roles. One is to protect and stabilize the Cu_2O nanocubes, and prevent the nanocrystals from aggregation. The other is that these composite structures prohibit the combination of electron–hole pairs and facilitate interfacial charge transfer. Using this way, we could synthesize other metal oxide or metal composite in further studies.

Acknowledgments

This work was supported by the National Natural Science Foundation of China (Nos. 21073031, 20573017 and 20803008) and Analysis and Testing Foundation of Northeast Normal University.

Appendix A. Supplementary Information

Supplementary data associated with this article can be found in the online version at doi:10.1016/j.jssc.2011.03.055.

References

[1] D. Jiang, Y. Xu, D. Wu, Y.H. Sun, J. Solid State Chem. 181 (2008) 593–602.
[2] E.S. Jang, J.H. Won, Y.W. Kim, Z. Cheng, J.H. Choy, J. Solid State Chem. 183 (2010) 1835–1840.
[3] A.O. Musa, T. Akomolafe, M.J. Carter, Sol. Energy Mater. Sol. Cells 51 (1998) 305–316.
[4] X. Li, F.F. Tao, Y. Jiang, Zh. Xu, J. Colloid Interface Sci. 308 (2007) 460–465.
[5] K.R. Reddy, B.C. Sin, C.H. Yoo, W. Park, K.S. Ryu, J.S. Lee, D. Sohnc, Y. Lee, Scr. Mater. 58 (2008) 1010–1013.
[6] W.W. Zhou, B. Yan, C.W. Cheng, C.X. Cong, H.L. Hu, H.J. Fan, T. Yu, Cryst. Eng. Commun. 11 (2009) 2291–2296.
[7] M.H. Kim, B. Lim, E.P. Lee, Y.N. Xia, J. Mater. Chem. 18 (2008) 4069–4073.
[8] Z.Z. Chen, E.W. Shi, Y.Q. Zheng, W.J. Li, B. Xiao, J.Y. Zhuang, J. Cryst. Growth 249 (2003) 294–300.
[9] H.L. Xu, W.Z. Wang, W. Zhu, J. Phys. Chem. B 110 (2006) 13829–13834.
[10] M.H. Cao, C.W. Hu, Y.H. Wang, Y.H. Guo, C.X. Guo, E.B. Wang, Chem. Commun. (2003) 1884–1885.
[11] Y.S. Luo, S.Q. Li, Q.F. Ren, J.P. Liu, L.L. Xing, Y. Wang, Y. Yu, Z.J. Jia, J.L. Li, Cryst. Growth Des. 7 (2007) 87–92.
[12] C. Xu, X. Wang, L.C. Yang, Y.P. Wu, J. Solid State Chem. 182 (2009) 2486–2490.
[13] D.B. Wang, M.S. Mo, D.B. Yu, L.Q. Xu, F.Q. Li, Y.T. Qian, Cryst. Growth Des. 3 (2003) 717–720.

[14] Y.S. Luo, Y.C. Tu, Q.F. Ren, X.J. Dai, L.L. Xing, J.L. Li, J. Solid State Chem. 182 (2009) 182–186.
[15] Y.G. Zhang, L.L. Ma, J.L. Li, Y. Yu, Environ. Sci. Technol. 41 (2007) 6264–6269.
[16] L.S. Zhang, J.L. Li, Z.G. Chen, Y.W. Tang, Y. Yu, Appl. Catal. A 299 (2006) 292–297.
[17] B. Zhou, Z.G. Liu, H.X. Wang, Y.Q. Yang, W.H. Su, Catal. Lett. 132 (2009) 75–80.
[18] A. Zahoor, T. Qiu, J.R. Zhang, X.Y. Li, J. Mater. Sci. 44 (2009) 6054–6059.
[19] P.S. Abthagir, R. Saraswathi, Thermochim. Acta 424 (2004) 25–35.
[20] J.V. Grazulevicius, I. Soutar, L. Swanson, Macromolecules 31 (1998) 4820–4827.
[21] A.D.D. Dwivedi, A.K. Singh, R. Prakash, P. Chakrabarti, Adv. Optoelectr. Mater. Dev. (2008) 56–64.
[22] Z.M. Zhang, J.Y. Deng, J. Sui, L.M. Yu, M.X. Wan, Y. Wei, Macromol. Chem. Phys. 207 (2006) 763–769.
[23] Y.M. Sui, W.Y. Fu, H.B. Yang, Y. Zeng, Y.Y. Zhang, Q. Zhao, Y.G. Li, X.M. Zhou, Y. Leng, M.H. Li, G.T. Zou, Cryst. Growth Des. 10 (2010) 99–108.
[24] A. Zahoor, T. Qiu, J.R. Zhang, X.Y. Li, J. Mater. Sci. 44 (2009) 6054–6059.
[25] B. Gupta, R. Prakash, Synth. Met. 160 (2010) 523–528.
[26] Z.C. Orel, A. Anlovar, G. Drai, M. igon, Cryst. Growth Des. 7 (2007) 453–458.
[27] L. Huang, F. Peng, H. Yu, H.J. Wang, Solid State Sci. 11 (2009) 129–138.
[28] R. Flamia, G. Lanza, A.M. Salvi, J.E. Castle, A.M. Tamburro, Biomacromolecules 6 (2005) 1299–1309.
[29] H. Taoud, J.C. Bernede, A. Bonnet, M. Morsli, A. Godoy, Thin Solid Films 304 (1997) 48–55.
[30] S.Y. Abe, J.C. Bernéde, L. Ugalde, Y. Trégouët, M.A. del Valle, J. Appl. Polym. Sci. 106 (2007) 1568–1575.
[31] J.L. Li, L. Liu, Y. Yu, Y.W. Tang, H.L. Li, F.P. Du, Electrochem. Commun. 6 (2004) 940–943.
[32] J.Y. Ho, M.H. Huang, J. Phys. Chem. C 113 (2009) 14159–14164.
[33] U. Riaz, S.M. Ashraf, Appl. Clay Sci. 52 (2011) 179–183.
[34] Z.K. Zheng, B.B. Huang, Z.Y. Wang, M. Guo, X.Y. Qin, X.Y. Zhang, P. Wang, Y. Dai, J. Phys. Chem. C 113 (2009) 14448–14453.